Boundary-Layer Meteorol (2008) 129:451–468
DOI 10.1007/s10546-008-9327-5

ORIGINAL PAPER

Relaxed Eddy Accumulation Simulations of Aerosol Number Fluxes and Potential Proxy Scalars

Andreas Held · Edward Patton · Luciana Rizzo · Jim Smith · Andrew Turnipseed · Alex Guenther

Received: 24 April 2008 / Accepted: 6 October 2008 / Published online: 29 October 2008

Abstract Direct eddy-covariance measurements of aerosol number fluxes obtained during the 2007 CHATS field experiment in Dixon, California, USA are compared with relaxed eddy accumulation simulations using temperature and water vapour concentration as proxy scalars. After a brief discussion of the limited time response of the aerosol measurement, the applicability of temperature and water vapour concentration as proxy scalars for aerosol number concentration is investigated by evaluating scalar and spectral correlation coefficients as simple measures of scalar similarity. In addition, the proportionality factor b, which compensates for the use of a constant sampling flow in relaxed eddy accumulation, is derived from the time series of aerosol number, temperature and water vapour, and its variability is analyzed. The reduction of the b factor due to application of a deadband, i.e. the rejection of data when the vertical wind speed is close to zero, is evaluated for all three studied scalars, and compared with published functional relationships. In this study, using temperature or water vapour as proxy scalars for aerosol number shows no advantage over the use of a constant b factor. Thus, it is suggested to apply a deadband $H_{REA} = w'/\sigma_w = 0.6$ to 0.8 (where w' is the vertical velocity fluctuation and σ_w is its standard deviation), to use a theoretical b factor based on a parameterization that includes a stability dependence, and to calculate the deadband effect according to a derived relation for aerosol relaxed eddy accumulation.

Keywords Aerosol number flux · Eddy covariance · Relaxed eddy accumulation · Scalar similarity

A. Held (✉) · L. Rizzo · J. Smith · A. Turnipseed · A. Guenther
Atmospheric Chemistry Division, National Center for Atmospheric Research, Boulder, CO, USA
e-mail: held@ucar.edu

E. Patton
Mesoscale and Microscale Meteorology Division, National Center for Atmospheric Research, Boulder, CO, USA

1 Introduction

1.1 Aerosol REA

The vertical transport of aerosol particles in the atmospheric boundary layer has become an important research area in many scientific fields, e.g. in the context of aerosol-cloud–climate-interactions in atmospheric chemistry, or nutrient and pollutant input into ecosystems in biogeochemistry. The surface-atmosphere exchange in the boundary layer is primarily established through turbulent transport. Direct eddy-covariance measurements of vertical turbulent fluxes in the boundary layer require sufficiently fast sensors to determine the vertical wind speed and the investigated scalar concentration with a time resolution of typically 10 Hz. Therefore, eddy covariance is routinely applied mainly to measure the turbulent fluxes of momentum, sensible heat, water vapour, and CO_2 (e.g. Baldocchi et al. 2001). It has also been applied successfully to measure fluxes of trace gases such as ozone and volatile organic compounds, and aerosol number fluxes (e.g. Gallagher et al. 1997; Buzorius et al. 1998; Held and Klemm 2006). However, for many aerosol properties such as size-segregated number concentrations or constituent concentrations, fast sensors remain scarce. Fast optical particle counters have been used for size-segregated measurements of sea spray particles over the ocean (e.g. Norris et al. 2008). Nemitz et al. (2008) report a direct eddy covariance application of an aerosol mass spectrometer to measure chemical species fluxes. In the absence of sufficiently fast sensors, aerosol flux measurements are feasible through relaxed eddy accumulation (REA) (Businger and Oncley 1990), which is based on conditional sampling of atmospheric particles into separate reservoirs for updraft and downdraft air samples, and a comparison of the mean updraft and downdraft concentrations. Conditional sampling approaches have been reported for size-resolved aerosol flux measurements (Schery et al. 1998; Gaman et al. 2004; Grönholm et al. 2007), aerosol constituent fluxes (Nemitz et al. 2001; Held et al. 2003; Meyers et al. 2006; Myles et al. 2007), and as a post-processing procedure (Pryor et al. 2007).

The application of REA to measure atmospheric constituent fluxes in the field requires extensive real time data processing, including real time coordinate rotation of wind data and reliable spike removal. In addition to these REA-specific technical difficulties, it should be noted that the flux estimate from eddy covariance and REA does not take into account storage and advection of the scalar of interest. In order to arrive at reasonable surface-atmosphere exchange estimates, vertical and horizontal advection processes must be considered (e.g. Lee 1998; Aubinet et al. 2003).

An underlying assumption in REA is the similarity of the turbulent transport characteristics of different scalar quantities, e.g. temperature and aerosol number concentration. The validity of this assumption may be violated, for example, due to differences in atmospheric source and sink strengths of the scalars of interest. In a forest ecosystem, temperature variations are mainly determined by the heating of air at the top of the canopy during the day and reduced cooling below the canopy during the night. In contrast, aerosol particles are effectively removed from the atmosphere in the canopy through impaction and interception processes, while secondary aerosol formation is a potential particle source, usually considered to be located above the canopy (Held et al. 2004). Other potential aerosol sources may be re-suspension of mineral dust from the soil or mechanical abrasion of particles from surfaces in the canopy.

Active scalars such as temperature and to a certain degree water vapour actively influence turbulent exchange, whereas passive scalars such as carbon dioxide do not produce or dissipate turbulent kinetic energy. Time series of reactive scalars (e.g. ozone) are influenced by

chemical reactions or transformations on time scales relevant to turbulent exchange. REA is not applicable if these changes take place on the same time scale as vertical velocity sampling (Katul et al. 1996). With regard to aerosol number fluxes, the aerosol number concentration may change due to coagulation and scavenging processes, therefore exhibiting non-stationary behaviour more frequently than other scalars. Thus, we consider the aerosol number concentration to be a reactive scalar, however, with reaction time scales slow enough (min to hours) to allow the application of REA.

1.2 REA Theory

REA (Businger and Oncley 1990) is a variant of the eddy accumulation method (Desjardins 1977), which separates air samples into updraft and downdraft reservoirs according to the direction and magnitude of the vertical wind. In principle, the turbulent flux of an atmospheric constituent can be determined from the concentration difference between the two reservoirs when the flow rate into the reservoirs is kept proportional to the vertical wind speed. Hicks and McMillen (1984) tested the applicability of this method for measuring pollutant fluxes numerically.

However, a technical implementation of the requirement to sample with a flow rate proportional to the vertical wind speed is hard to realize. Therefore, this requirement may be "relaxed" in REA by keeping the flow rate constant, while compensating for the loss of information through flux-variance similarity assumptions and the introduction of a proportionality factor b. Then, the flux F_{REA} is calculated according to

$$F_{REA} = b\sigma_w(c_{up} - c_{down}), \tag{1}$$

with b, a proportionality factor, σ_w is the standard deviation of the vertical wind speed, and $c_{up} - c_{down}$ is the scalar concentration difference between the updraft and downdraft reservoirs, typically averaged over a period of 30 min. Pattey et al. (1993) showed that REA is a good approximation to a flux integration based on the vertical wind velocity.

For an ideal Gaussian joint probability distribution of the vertical wind speed and the scalar concentration, the proportionality factor b has a well-defined value of $b = 0.627$ (Wyngaard and Moeng 1992). Transport from organized motion alone yields a theoretical factor $b = 0.54$ (Katul et al. 1996). However, experimentally determined b factors for fluxes of heat, moisture and CO_2 typically range from 0.51 to 0.62 (e.g., Katul et al. 1996). Moreover, for individual 30-min averaging periods, significant variations of b have been reported indicating that b may not be considered a universal constant.

Therefore, the proportionality factor b is often derived from a scalar quantity, for which the turbulent flux F_{EC} can be determined by eddy covariance as the covariance of the vertical wind speed w and the scalar c,

$$F_{EC} = \overline{w'c'}. \tag{2}$$

Equating F_{REA} and F_{EC} and rearranging Eqs. 1 and 2 yields the proportionality factor b from

$$b = \frac{\overline{w'c'}}{\sigma_w(\overline{c_{up}} - \overline{c_{down}})} \tag{3}$$

Obviously, the use of b derived from a proxy scalar different from the scalar studied in REA requires scalar similarity, which can be evaluated by comparing the time series and spectra of the two scalars (Kaimal et al. 1972; Pearson et al. 1998).

In practical REA systems, air samples are commonly discarded when fluctuations of the vertical wind speed are close to zero. This wind deadband, defined by an arbitrary upper and

lower threshold of the vertical wind speed around zero, significantly reduces the frequency of valve switching, and increases the scalar concentration difference. A greater concentration difference between the two reservoirs also reduces errors due to uncertainties in the determination of updraft and downdraft scalar concentrations.

In REA, the wind deadband H_{REA} is usually scaled with the standard deviation of the vertical wind speed, yielding the following dynamic definitions of updrafts and downdrafts:

updraft:

$$H_{REA} < \frac{w'}{\sigma_w}, \tag{4a}$$

downdraft:

$$-H_{REA} > \frac{w'}{\sigma_w}. \tag{4b}$$

In the so-called hyperbolic relaxed eddy accumulation (Bowling et al. 1999), the hyperbolic deadband H_{HREA} defines thresholds that exclude samples both when fluctuations of the vertical wind speed or the scalar concentration are small:

updraft:

$$H_{HREA} < \frac{w'c'}{\sigma_w \sigma_c}, \tag{5a}$$

downdraft:

$$-H_{HREA} > \frac{w'c'}{\sigma_w \sigma_c} \tag{5b}$$

Depending on the selected deadband, the sampling process is concentrated towards strong updrafts and downdrafts, increasing the scalar concentration difference between the updraft and downdraft reservoir and, at the same time, increasing the skewness of the joint probability distribution. The corresponding b value is reduced in order to compensate for these changes. Functional relationships of the reduction of b have been suggested for various scalars including temperature, CO_2, and water vapour (Businger and Oncley 1990; Pattey et al. 1993; Ammann and Meixner 2002) but not for aerosol number concentrations. It is important to bear in mind that these functional relationships only represent adjustments of average b values and cannot reflect variations during individual averaging periods. This variation may be achieved by use of a proxy scalar to derive individual b values. However, good scalar similarity is required, especially in hyperbolic REA, where the proxy scalar is also used in the definition of the hyperbolic deadband (cf. Eq. 5a, b).

In REA calculations, uncertainties in the b factor due to a lack of similarity between the scalar of interest and the proxy scalar translate linearly into the overall uncertainty of the REA flux estimate. In the present study, eddy-covariance measurements of aerosol number fluxes are compared with relaxed eddy accumulation simulations using temperature and water vapour concentration as proxy scalars. To evaluate the quality of these simulations, the scalar similarity of the aerosol number concentration and the two potential proxy scalars is investigated. Additionally, theoretical b values using different deadband definitions are applied and the optimum deadband definition is evaluated.

2 Methods

2.1 Site and System

Turbulent time series of temperature, water vapour and particle number concentration were obtained during the Canopy Horizontal Array Turbulence Study (CHATS) in May 2007 at Cilker Orchards, Dixon, California, USA. An eddy-covariance system consisting of a CSAT3 sonic anemometer (Campbell Scientific, Logan, UT, USA) and a CPC 3772 condensation particle counter (TSI, St. Paul, MN, USA) was set up on a 30-m meteorological tower at 14 m agl in a walnut orchard with an average height of about 9 m and a homogeneous canopy structure. The trees were about 25 years old and planted in a nearly-square pattern of 7 m by 7 m. The plant area index was about 2.5, with a distinct maximum of the plant area density in the top 2 m of the moderately rough walnut canopy. Further details on the CHATS experiment and measuring site can be found in Patton et al. (*to be submitted to the Bulletin of the American Meteorological Society*).

The closest edge of the orchard was 123 m to the north of the tower, with agricultural land, mostly freshly ploughed tomato fields, adjacent. The opposite edge of the orchard was approximately 1.5 km south of the tower. Additionally, water vapour measurements were made with a KH20 krypton hygrometer (Campbell Scientific, Logan, UT, USA) at the same sampling height. The sonic anemometer and the hygrometer were mounted on a boom facing west, while the condensation particle counter (CPC) was located in an enclosure on the tower. Aerosol particles were sampled 0.7 m behind and slightly below the sonic anemometer measurement region and transported to the particle counter through 2.6 m of conductive tubing with an inner diameter of 7.9 mm. The flow rate through the sampling line was $1.01\,\mathrm{l\,min^{-1}}$, thus establishing laminar flow. This leads to a degraded response time of the particle counter with regard to ambient concentration changes. While submicron particle losses in the sampling line due to gravitational settling are negligible, diffusional losses of 10 nm particles may be as high as 20% (Willeke and Baron 1996).

In the field, the total number concentration of particles in the diameter range from 10 nm to 3 µm was sampled at 10 Hz, while all other data were sampled with a time resolution of 60 Hz. It should be noted that the actual response time (1/e signal change) of the CPC is estimated to be $t = 0.42$ s, and the response time of the CPC including the sampling line is estimated to be $t = 0.61$ s. These time constants were determined experimentally by fitting a first-order response function to concentration step changes, and confirmed in spectral analyses of field data. A 95% response of the particle counter to a signal change is reached after three times these values. The CPC is a single-particle counting instrument detecting each particle individually for number concentrations below $10000\,\mathrm{cm^{-3}}$, when coincidence of particles in the detection volume is not an issue. For higher particle concentrations, a coincidence correction is applied. The uncertainty of the eddy covariance estimate of the deposition velocity due to poor counting statistics was evaluated according to Buzorius et al. (2003), and was less than $0.5\,\mathrm{mm\,s^{-1}}$ during the entire measurement period.

For further analysis, all data were re-sampled and synchronized with a time resolution of 10 Hz. The shift between the aerosol number concentration and all other data caused by the sampling line delay was evaluated with a cross-correlation analysis maximizing the covariance between the aerosol number concentration and the vertical wind speed. This analysis yielded a relatively constant time lag of 3.6 s, which is in good agreement with the theoretically expected value.

Aerosol number fluxes were measured during the second phase of the CHATS field experiment from May 14, 2007, to June 2, 2007, for a total of 18 days. From the evening

of May 23, 2007, through to the evening of May 25, 2007, sampling was suspended for a scheduled insecticide treatment of the orchard. During most of the remaining period, a very distinct diurnal pattern of shifting wind direction was observed. Typically, strong winds from the south prevailed at night, with lighter winds from the north and north-west during the day. The pronounced transition between daytime and nighttime wind conditions usually took place at 0600 Pacific Daylight Time (PDT) in the morning and around 1600 PDT in the afternoon. On several days, no shift in wind direction was observed and extended periods of constant wind flow could be analyzed. For this study, two consecutive days (May 21 and 22) with steady winds from the north and north-west were selected. Due to sensor failure, the water vapour measurement is only available starting at 1300 PDT on May 21.

2.2 Data Analysis

Turbulent fluxes were calculated according to standard eddy-covariance procedures for 30-min averaging periods. Coordinate rotation was applied to all wind data using the planar fit method (Wilczak et al. 2001). Unless noted otherwise, the time series were not detrended. The friction velocity u_* was calculated as the square root of the momentum flux,

$$u_* = \sqrt{-\overline{u'w'}}, \tag{6}$$

and the stability parameter z/L was calculated using $z = 9\,\mathrm{m}$, and the Obukhov length,

$$L = \frac{-u_*^3}{\kappa(g/T)\overline{w'T'}}. \tag{7}$$

Here κ is the von Karman constant, g is the gravitational acceleration [m s^{-2}], T is temperature [K]. The aerosol deposition velocity v_d was calculated as the negative normalized aerosol number flux,

$$v_d = -\frac{\overline{w'c'}}{c}. \tag{8}$$

Positive v_d values indicate particle deposition, while negative v_d values correspond to particle emission.

REA and hyperbolic REA sampling was simulated by segregating data into updraft and downdraft reservoirs according to the vertical wind speed fluctuation, using the deadband definitions of REA (Eq. 4a, b) and hyperbolic REA (Eq. 5a, b), respectively. With eddy-covariance calculations as a reference, the corresponding b factors were derived from Eq. 3.

As a simple measure to evaluate the similarity of the time series of aerosol number concentration, sonic temperature and water vapour, the scalar correlation coefficient r between the two scalars of interest, c_1 and c_2,

$$r = \frac{\overline{c_1' c_2'}}{\sigma_{c_1}\sigma_{c_2}} \tag{9}$$

was calculated. This approach has been used by Gao (1995), Katul and Hsieh (1999) and Ruppert et al. (2006) to investigate the scalar similarity between temperature, water vapour and CO_2.

While the scalar correlation coefficient integrates over all frequencies, the similarity of time series in specific frequency ranges may be analyzed using a spectral correlation

coefficient r_s. In this study, r_s was calculated from the real and imaginary parts, Re and Im, of the Fourier coefficients of a Fourier transform of the two time series of interest,

$$r_s = \frac{\sum(\mathrm{Re}_1\mathrm{Re}_2 + \mathrm{Im}_1\mathrm{Im}_2)}{\sqrt{\sum\left(\mathrm{Re}_1^2 + \mathrm{Im}_1^2\right)\sum\left(\mathrm{Re}_2^2 + \mathrm{Im}_2^2\right)}} \tag{10}$$

The spectral correlation coefficient was evaluated in three frequency ranges from 0.333 to 3.333 Hz (high frequency range with a characteristic time scale of 0.3 to 3 s), 0.0333 to 0.333 Hz (medium frequency range, 3 to 30 s), and 0.0033 to 0.0333 Hz (low frequency range, 30 to 300 s).

3 Results and Discussion

3.1 Flux Measurements

On May 21 and 22, 2007, low-level flow was continuously from the north and north-west directions at wind speeds typically around 6 to 7 m s^{-1} during daytime, and 1 to 3 m s^{-1} during the night. In order to characterize the two-day dataset used for further analysis, Fig. 1 shows the temporal evolution of air temperature, the relative humidity, wind speed, the atmospheric stability z/L, the buoyancy heat flux, the friction velocity u_*, aerosol number concentration, aerosol number flux, and aerosol deposition velocity.

Both temperature and relative humidity (Fig. 1a) follow a clear diurnal cycle: the air temperature reaches about 28°C in the late afternoon and falls below 20°C during the night and early morning. The relative humidity is low during daytime (typically < 20 %) and higher during the night. On May 21, the wind speed (Fig. 1b) increases to a maximum of about 8 m s^{-1} at noon, while it stays relatively constant around 6 m s^{-1} on May 22. For most of the two-day period, near-neutral or slightly unstable atmospheric conditions prevail (cf. Fig. 1b), especially during daytime from 0800 to 1800 PDT when the largest turbulent fluxes are observed. Stable conditions are encountered on May 21 from 0000 to 0800 PDT and from 2100 to 2330 PDT. The buoyancy heat flux (Fig. 1c) was calculated as the covariance of vertical wind speed and sonic temperature. It exhibits a clear diurnal pattern with slightly negative values during the night and a positive maximum slightly after noon around 1300 PDT. The friction velocity (Fig. 1d) is greater than 1 m s^{-1} for most of the time, indicating well-developed turbulent transport above the canopy.

The total aerosol number concentration (Fig. 1e) exhibits a steep increase in the morning starting around 1000 PDT, peaks at 1400 PDT as high as 25,000 particles cm^{-3}, and drops again to nighttime background values of 3,000–4,000 cm^{-3} at 1800 PDT. The turbulent aerosol number flux (Fig. 1f) exhibits a clear diurnal pattern. In the morning, aerosol emission fluxes are observed when turbulent transport (as indicated by the buoyancy heat flux pattern) sets in. The onset of aerosol deposition at 1000 PDT is clearly correlated with the increase in aerosol number concentration at the same time. Aerosol deposition fluxes peak around 1300 PDT, decrease to values close to zero at 1900 PDT, and remain negligible during the night.

The aerosol deposition velocity v_d (cf. Eq. 8) in Fig. 1g is close to zero at night and drops to negative values during the brief emission periods in the morning. The highest v_d values (30–40 mm s^{-1}) are observed early during aerosol deposition, before slowly decreasing in the afternoon to background values in the evening and night. Note that particle emission is indicated by positive aerosol fluxes yet negative deposition velocities v_d, while particle deposition yields negative aerosol fluxes and positive deposition velocities.

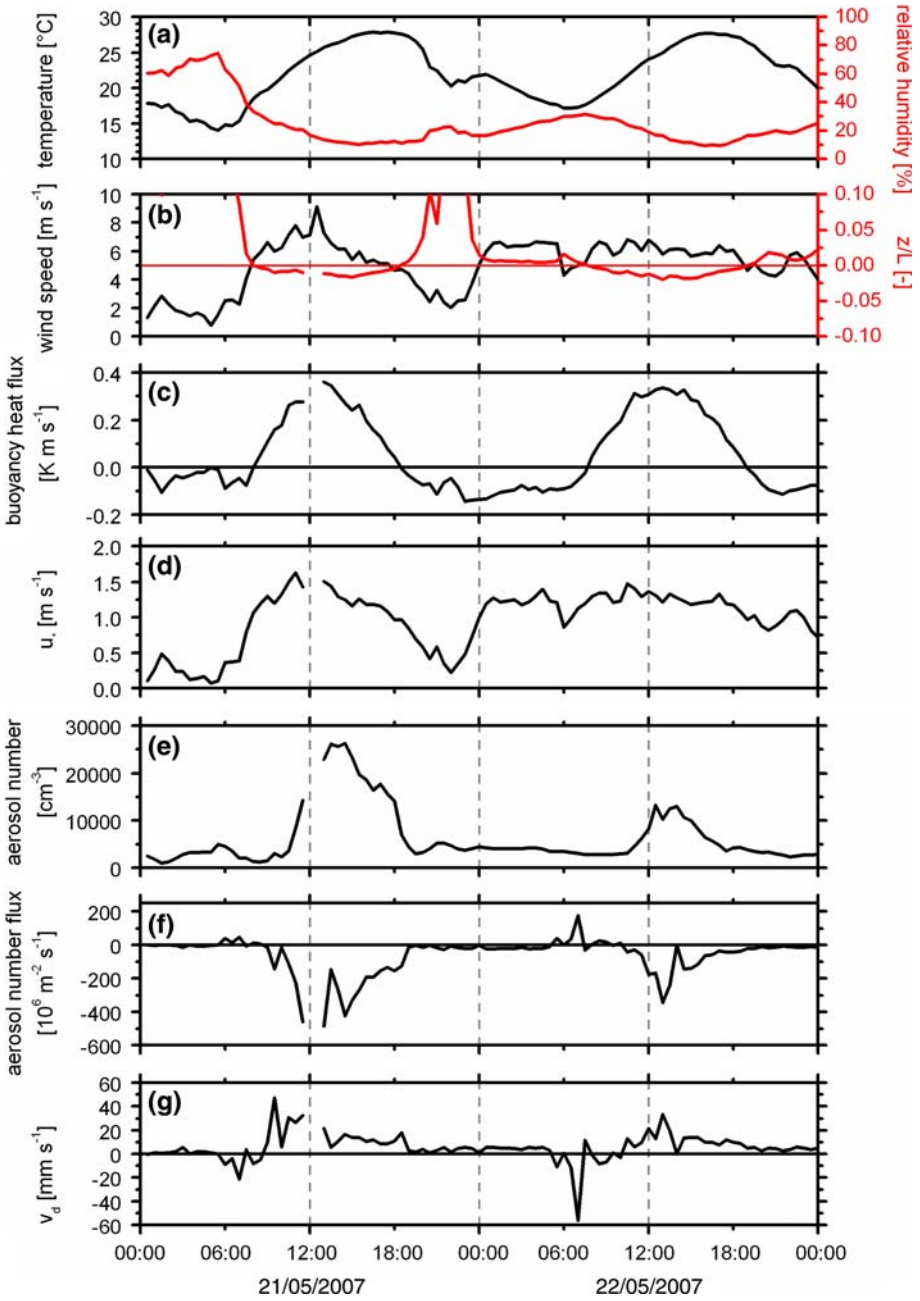

Fig. 1 **(a)** Air temperature and relative humidity, **(b)** wind speed and atmospheric stability z/L, **(c)** buoyancy heat flux, **(d)** friction velocity u_*, **(e)** aerosol number concentration, **(f)** aerosol number flux, and **(g)** aerosol deposition velocity v_d measured on May 21 and 22, 2007, during the CHATS field experiment, Dixon, CA, USA using 30-min averaging periods. All data were measured at a height of 14 m agl

The observed aerosol number flux appears to be a composite of two distinct particle transport mechanisms: emission fluxes when turbulent transport becomes effective in the morning and low particle number concentrations at the same time may be explained by extensive farming activities on relatively dry soil north of the walnut orchard. Suspended dust was visible in the morning on both days, but did not significantly increase the number concentration. Therefore, mechanical re-suspension of soil must be considered a source of rather large particles, which may contribute to a high particle mass loading, but not to a substantial increase in particle number. Later in the morning, a steep increase in particle number was associated with strong particle deposition. While the source of the particles contributing to elevated number concentrations may be local (e.g. particle formation) or remote (and subsequently advected), the high number concentration and the high deposition velocity indicate that very small particles (<100 nm diameter) dominate the aerosol number flux under these conditions. The deposition velocity is strongly size-dependent, with a minimum in the accumulation range (100–1000 nm diameter) and increasing deposition velocities for smaller and larger particles. The deposition flux of many small particles may mask continued emission of larger, but fewer dust particles. The slowly decreasing trend of the deposition velocity during the day is consistent with increasing particle diameters, e.g. due to condensational growth of organic vapours (cf. Held et al. 2006). In order to unambiguously separate these processes, size-resolved aerosol flux measurement capabilities are required in future experimental studies.

In order to evaluate the limited response of the condensation particle counter to changes in aerosol number concentration, Fig. 2 displays a comparison of aerosol number fluxes (Fig. 2a), buoyancy heat fluxes (Fig. 2b), water vapour fluxes (Fig. 2c), and momentum fluxes (Fig. 2d) derived from the original 10 Hz time series and from time series re-sampled at 2, 1 and 0.5 Hz, respectively.

At lower time resolution, high frequency flux contributions from small-scale turbulence are not resolved, and the corresponding flux estimates are expected to be systematically lower. This can be clearly observed in the buoyancy heat flux, the water vapour flux, the momentum flux, and also, to a lesser extent, in the aerosol flux data. The systematic reduction of the turbulent fluxes is described by the slope of the linear regression functions in Fig. 2, where the offsets of all regression functions can be considered negligible. In the case of the aerosol number fluxes, the regression slope is just slightly lower than 1 when using 2 Hz data, 0.971 when using 1 Hz data, and 0.889 when using 0.5 Hz data. In all other cases, the slopes are 0.92–0.94 when using 2 Hz data, 0.84–0.87 when using 1 Hz data, and 0.69–0.73 when using 0.5 Hz data. The latter results are consistent with the flux reduction due to fluctuation dampening as described by Horst (1997). The larger scatter and smaller flux reduction in the aerosol case may be attributed to the limited response time of the CPC, which does not fully resolve the aerosol number concentration with a time resolution of 10 Hz.

The scalar similarity of the aerosol number concentration and temperature or water vapour concentration is generally low. Figure 3 shows the scalar and spectral correlation coefficients of the aerosol number concentration and the two potential proxy scalars.

The absolute value of the scalar correlation coefficient of aerosol number concentration (Fig. 3a, c) typically ranges from $r = 0$ to 0.5, while only a few periods with higher scalar correlation coefficients can be found. The absolute r_S values of aerosol number concentration (Fig. 3b, d) are smaller than 0.1 in the high frequency range for most of the time. This is expected because the high frequency range is not fully resolved with the condensation particle counter. In the medium and low frequency ranges, fair correlation can be observed with a clear diurnal pattern. The correlation between aerosol number concentration and temperature is usually positive during the night and negative during the day, while in the case of water

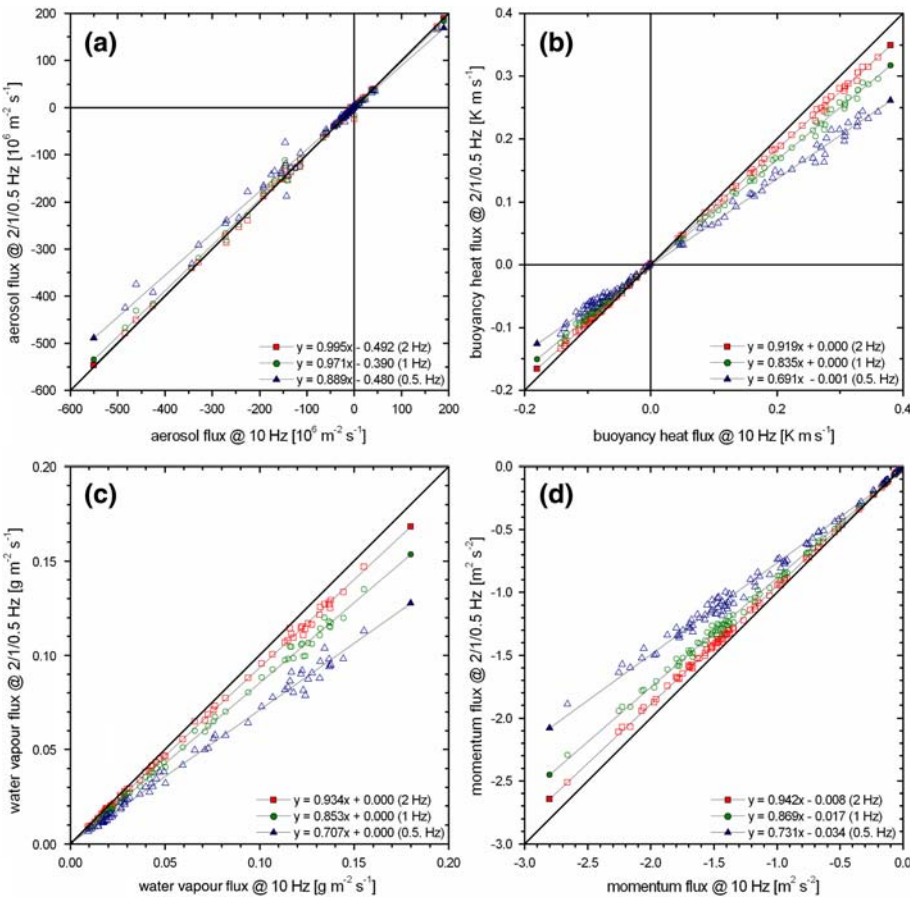

Fig. 2 Scatter plot of **(a)** aerosol number fluxes, **(b)** buoyancy heat fluxes, **(c)** water vapour fluxes, and **(d)** momentum fluxes derived from the original 10 Hz time series, and from time series re-sampled at 2 Hz (red), 1 Hz (green), and 0.5 Hz (blue). Linear regression functions are given in each panel

vapour concentration the spectral correlation coefficient remains negative for most of the time. In particular, the r_s values in the medium frequency range are strongly anti-correlated during the night, and positively correlated during the day. Temperature and water vapour concentration (Fig. 3e, f) show generally high absolute correlation coefficients in all three frequency ranges, i.e. strong correlation during the day and strong anti-correlation during the night. Clearly, the low similarity of aerosol number concentration and the two potential proxy scalars in the high frequency range lower the overall scalar similarity and considerably affect the scalar correlation coefficient.

3.2 REA and Hyperbolic REA Simulations

In REA and hyperbolic REA, the fraction of the data that falls between the limits of the updraft and downdraft definitions close to zero is discarded. Therefore, the total sample volume ΔS (or the total number of data points) decreases with increasing deadband values H. On the other hand, the application of a wind deadband increases the scalar concentration difference

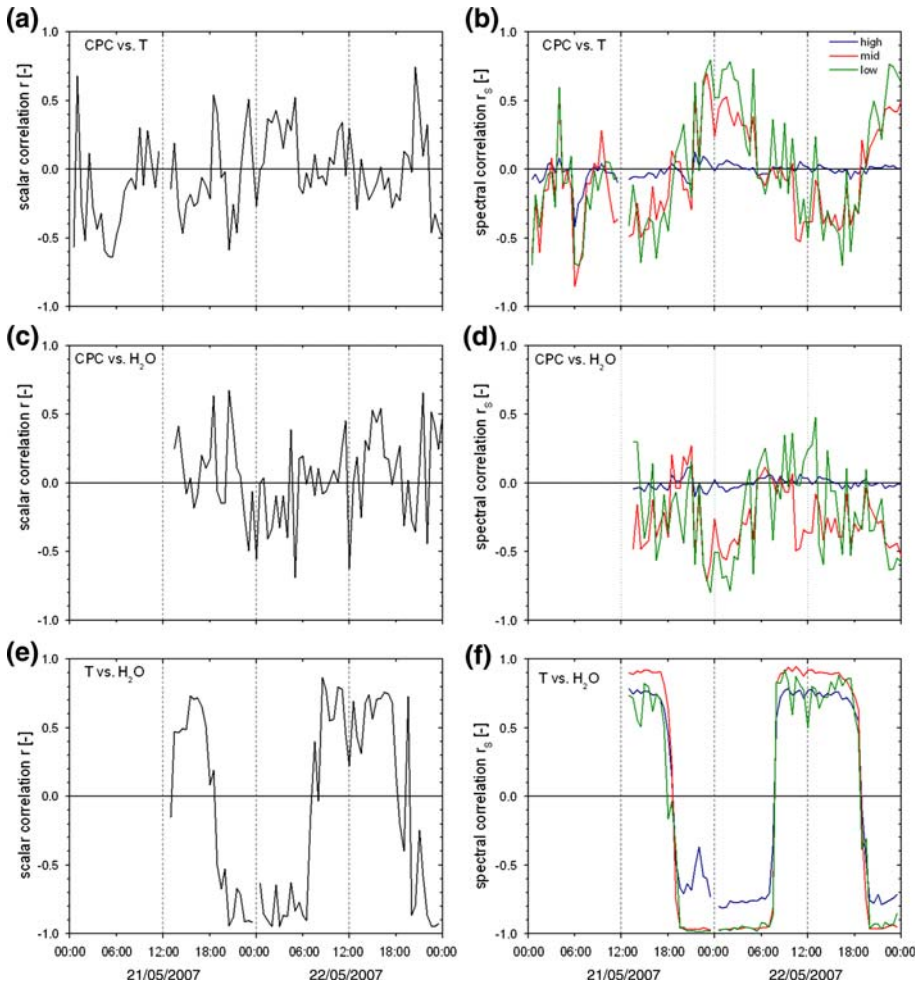

Fig. 3 **(a, c, e)** Scalar correlation coefficient r between aerosol number concentration, temperature and water vapour concentration, and **(b, d, f)** spectral correlation coefficients r_S between aerosol number concentration, temperature and water vapour concentration in three frequency ranges (0.333–3.333 Hz: blue, 0.0333–0.333 Hz: red, 0.0033–0.0333 Hz: green)

ΔC because the sampling process is shifted towards stronger updrafts and downdrafts. For a given analytical system measuring the updraft and downdraft concentration averages, this may restrict or encourage the use of a certain deadband value. If the accuracy of the analytical system is the limiting factor, it is favourable to increase the concentration difference by increasing the wind deadband. If, however, the sensitivity of the analytical system is a limiting factor, it is favourable to keep a large sample volume that is sufficient to reliably analyze the updraft and downdraft concentration averages. If the sensitivity and accuracy of the analytical system allow the application of a deadband range, the optimum deadband (from an analytical perspective) is defined by a combination of the concentration difference increase and the sample volume reduction.

Table 1 Median values of the updraft and downdraft time fractions (T_{up} and T_{down}), sample fraction ΔS, i.e. the sum of T_{up} and T_{down}, the increase in the aerosol number concentration difference ΔC between updrafts and downdrafts, and the product of ΔS and ΔC of the individual half-hour periods of the two-day data set (May 21 and 22, 2007) for deadband values H_{REA} ranging from 0 to 1

H_{REA}	T_{up}	T_{down}	Sample fraction ΔS	Concentration diff ΔC	$\Delta C \cdot \Delta S$
0	0.501	0.499	1.000	1.000	1.000
0.1	0.459	0.462	0.921	1.082	0.997
0.2	0.421	0.423	0.844	1.158	0.978
0.3	0.382	0.384	0.767	1.215	0.932
0.4	0.346	0.347	0.693	1.294	0.897
0.5	0.311	0.311	0.623	1.360	0.847
0.6	0.277	0.277	0.554	1.390	0.770
0.7	0.245	0.244	0.489	1.431	0.700
0.8	0.214	0.213	0.427	1.489	0.636
0.9	0.185	0.185	0.370	1.509	0.558
1.0	0.159	0.159	0.318	1.525	0.485

Table 1 summarizes the updraft and downdraft time fractions of the two-day dataset for different deadband values, the total time fraction of data used for a given deadband, and the corresponding increase in the aerosol number concentration difference between updrafts and downdrafts. As an example, only 55.4% of the data is used for a deadband value $H_{REA} = 0.6$, while the concentration difference is increased to 139%. The increase of the concentration difference ΔC is inversely proportional to the reduction of the b factor in Eq. 1.

Figure 4a compares functional relationships proposed to describe the reduction of the b factor in REA depending on the selected deadband, and the median deadband effects for aerosol number concentration, temperature and water vapour concentration simulated in this study using Eq. 3. In the case of aerosol number, the reduction is less than in any other case, but a fit of the functional relationship by Pattey et al. (1993),

$$\frac{b_{\mathrm{REA}}}{b_0} = 1 - c(1 - \exp(-a H_{REA})) \tag{11}$$

with b_{REA}, the b factor using a deadband H_{REA}, and b_0, the b factor without a deadband, is in excellent agreement with the data using $c = 0.378$ and $a = 2.300$. This parameterization is similar to the one of Pattey et al. (1993) for CO_2 with $c = 0.412$ and $a = 2.125$. The reduction is larger for H_2O, and even larger for temperature, which is also the case for the parameterizations of Pattey et al. (1993). Overall, the observed reduction is smaller than proposed by Ammann and Meixner (2002) for neutral and unstable conditions. For comparison, the original parameterization of Businger and Oncley (1990), which is similar to the theoretical joint Gaussian distribution relationship as parameterized by Ammann and Meixner (2002), suggests a much larger reduction of b.

In the case of the hyperbolic relaxed eddy accumulation (Fig. 4b), the reduction of b is generally larger than in REA due to the concentration of the sampling process on the strongest updrafts and downdrafts. In contrast to Fig. 4a, the reduction is largest in the case of aerosol number concentration (b_{CPC}), and slightly less for temperature and water vapour concentration (b_{T} and $b_{\mathrm{H_2O}}$). All three cases show a stronger reduction than the deadband effect suggested by Bowling et al. (1999) for CO_2 data.

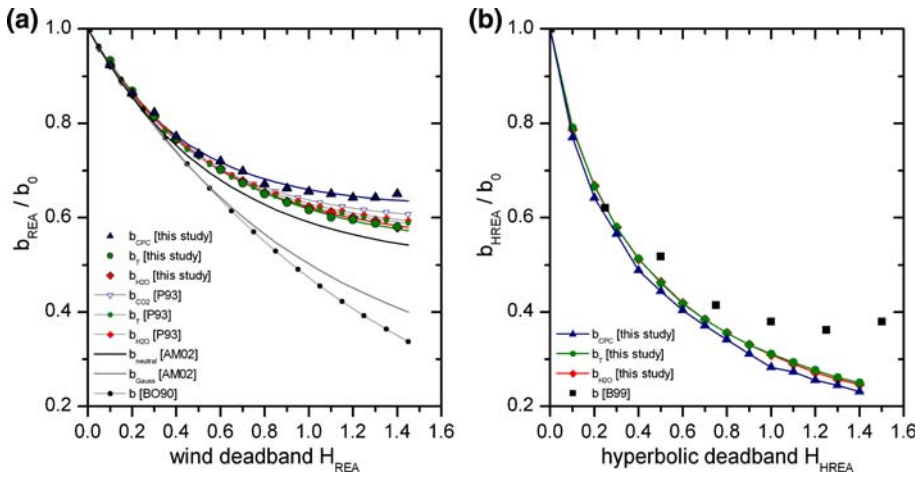

Fig. 4 Median reduction of the normalized b factor using different deadband values in **(a)** REA and **(b)** hyperbolic REA for aerosol number concentration (blue triangle), sonic temperature (green circle) and water vapour concentration (red diamond), and functional relationships or experimental data proposed for different scalars and conditions (P93: Pattey et al. 1993; AM02: Ammann and Meixner 2002; BO90: Businger and Oncley 1990; B99: Bowling et al. 1999). b_{REA} and b_{HREA} are normalized by b_0, the b factor without a wind deadband

Figure 5 shows the temporal evolution of b factors calculated according to Eq. 3 in 30-min intervals based on the 10 Hz time series of aerosol number concentration, sonic temperature, and water vapour concentration.

In Fig. 5a, c, e, no wind deadband was applied to simulate the updraft and downdraft separation. In the case of aerosol number concentration, the deviations from the median value $b_{\mathrm{CPC}} = 0.52$ seem random and much larger than for the temperature and water vapour cases. In fact, eleven data points deviate by more than 50 % from the median value, and a total of 20 data points is not displayed in Fig. 5a. In contrast, the b factors derived from temperature and water vapour appear to follow a diurnal pattern with higher values during the night and lower values at daytime. Andreas et al. (1998) and Ammann and Meixner (2002) have suggested elevated b factors under stable conditions, which is consistent with the present data. While the absolute values are lower in this study, the temporal pattern of the b factor is reproduced by a parameterization of the stability dependence (Ammann and Meixner 2002). In all three cases, linear detrending or autoregressive filtering of the original time series does not significantly reduce the observed scatter. In Fig. 5b, d, f, the updraft and downdraft definition was based on a wind deadband $H_{REA} = 0.6$. In the case of aerosol number concentration, ten data points deviate by more than 50% from the median value, and a total of 15 data points is not displayed in Fig. 5b. In general, the scatter is reduced, and the temporal patterns are still present yet less pronounced. This confirms previous studies, where a wind deadband $H_{REA} = 0.6$ to 0.8 was found to yield relatively stable b factors and small flux errors (Oncley et al. 1993; Foken et al. 1995; Ammann and Meixner 2002; Ruppert et al. 2006).

A different perspective that illustrates the advantage of a wind deadband in the range $H_{REA} = 0.6$ to 0.8 is presented in Fig. 6.

The box plot shows the relative deviation of b_{CPC}, i.e. the b factor derived from the aerosol number concentration time series, from b_{T} and $b_{\mathrm{H_2O}}$ as proxy scalars, and from a constant $b_{\mathrm{C}} = 0.52$ with a deadband effect according to Eq. 11 with $c = 0.378$ and $a = 2.3$, for different H_{REA} values. The line in the box represents the median deviation, the box limits are

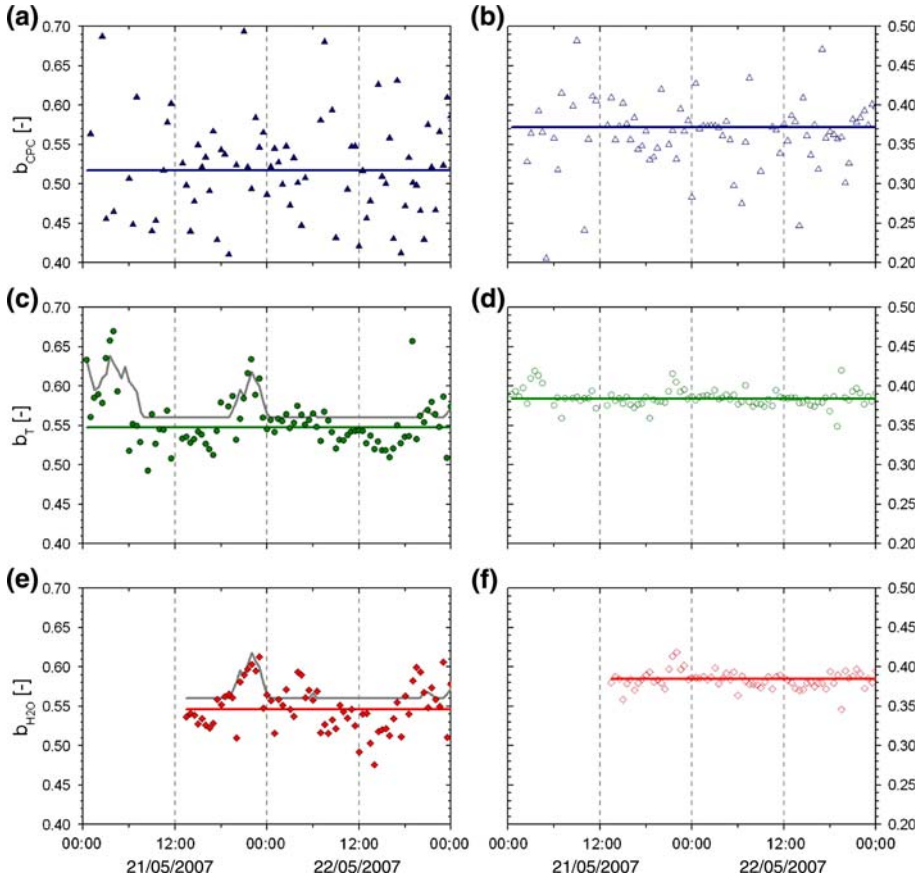

Fig. 5 b factors calculated for 30-min averaging periods: b_{CPC} derived from the aerosol number concentration **(a)** without deadband and **(b)** $H_{REA} = 0.6$, b_{T} derived from temperature **(c)** without deadband and **(d)** $H_{REA} = 0.6$, and $b_{\mathrm{H_2O}}$ derived from the water vapour concentration **(e)** without deadband and **(f)** $H_{REA} = 0.6$. Horizontal lines represent the median values of b, and grey lines in **(c)** and **(e)** represent a parameterization of the b factor depending on stability by Ammann and Meixner (2002)

the 25% and 75% percentiles of the deviations, and the diamonds give the 95% percentile (on a secondary axis) as a robust measure of the maximum deviation.

Comparing b_{CPC} with b_{T} (Fig. 6a), the median deviation is 10% to 15% for $H_{REA} = 0$ to 0.5, then drops below 10 % in the deadband range $H_{REA} = 0.6$ to 0.9, and rises again for $H_{REA} > 0.9$. Also, the interquartile range, i.e. the range of the middle 50% of the deviations, is relatively constant up to $H_{REA} = 0.5$, shows a distinct minimum for $H_{REA} = 0.7$ and 0.8, and increases for higher H_{REA}. The 95% percentile exhibits a distinct minimum at $H_{REA} = 0.6$ with a value of 82%. The same general observations are made when comparing b_{CPC} with $b_{\mathrm{H_2O}}$ (Fig. 6b) or a constant b_{C} (Fig. 6c). This clearly suggests that the application of a deadband in the range $H_{REA} = 0.6$ to 0.8 yields a fairly robust b factor. When the deadband is selected too small or too large, or a deadband is not applied at all ($H_{REA} = 0$), proxy scalar derived or parameterized b factors may deviate considerably from the b factor appropriate for the scalar of interest.

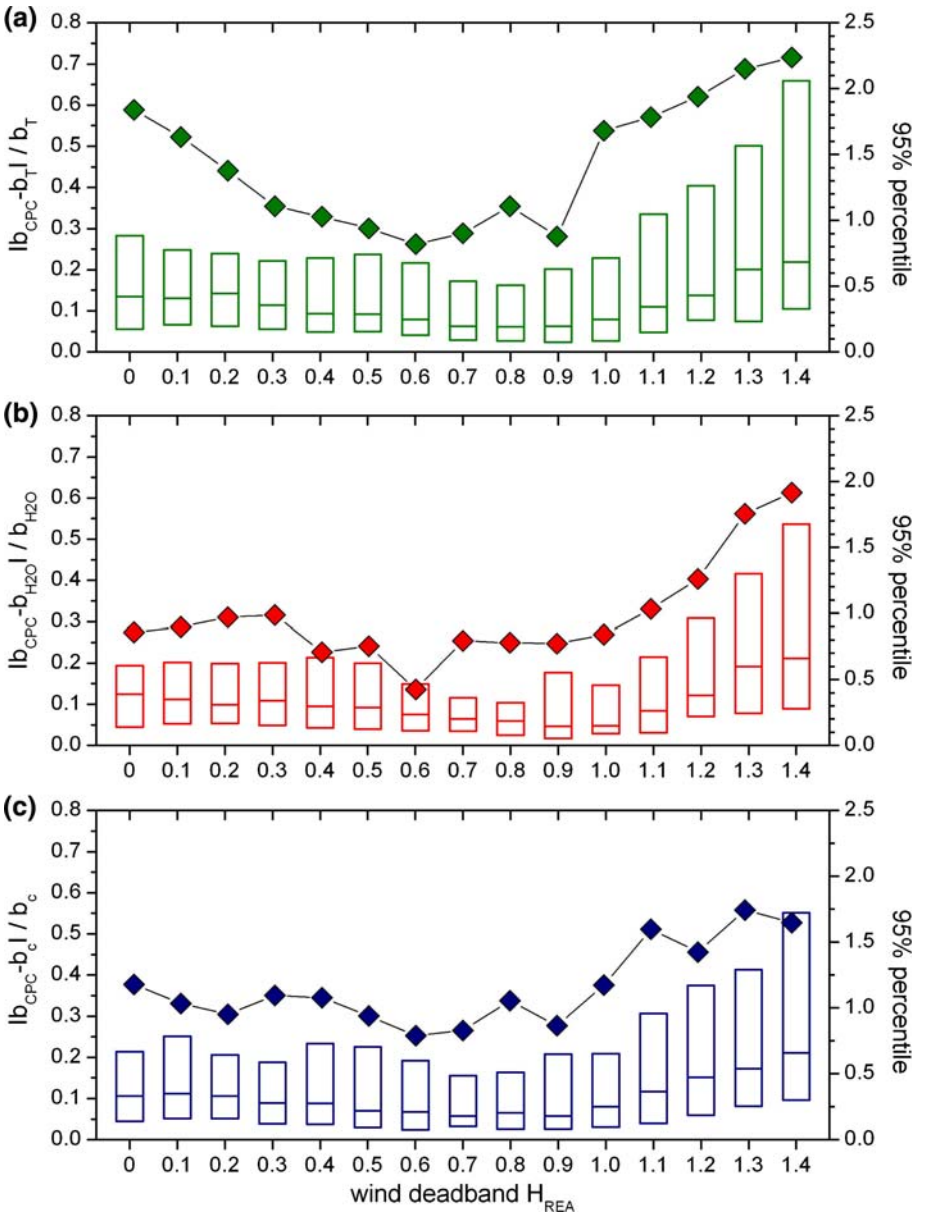

Fig. 6 Box plot of the relative deviation of b_{CPC} **(a)** from b_{T}, **(b)** from $b_{\mathrm{H_2O}}$ and **(c)** from a constant $b_{\mathrm{C}} = 0.52$ with a deadband effect according to Eq. 11 with $c = 0.378$ and $a = 2.3$. Box limits represent the 25% and 75% percentiles, the line in the box represents the median, and the diamonds represent the 95% percentile on the secondary axis to the right

As seen in Fig. 6, relative deviations of b factors derived from different proxy scalars can be large. However, the largest relative deviations are usually found when the turbulent fluxes are small, and when the relative uncertainty of the flux estimate is large. Thus, in this analysis different b factors do not contribute to a significant absolute deviation of the aerosol number flux estimates.

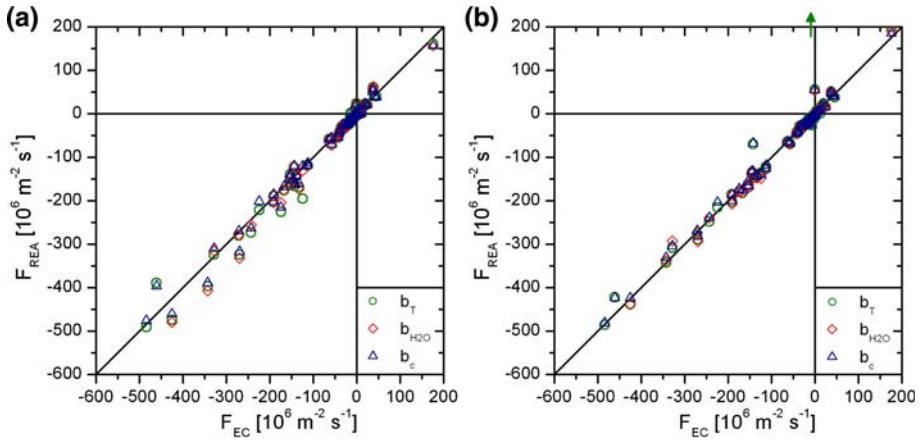

Fig. 7 Scatter plot of aerosol number fluxes measured directly by eddy covariance and estimated by REA simulations using b_T, b_{H_2O}, and a constant b_C for **(a)** $H_{REA} = 0$ (no deadband, $b_c = 0.52$) and **(b)** $H_{REA} = 0.6$ ($b_c = 0.37$). The green arrow in **(b)** indicates an individual outlier when using b_T

Figure 7 compares the aerosol number flux F_{EC} measured directly by eddy-covariance with the REA simulated flux estimates F_{REA} of the same dataset using b_T, b_{H_2O}, and a constant b_C for $H_{REA} = 0$ (Fig. 7a) and $H_{REA} = 0.6$ (Fig. 7b). Overall, the scatter is relatively minor, and using different b factors, the magnitude of the deviations is not significantly different from each other. Without applying a deadband, the REA simulations tend to slightly overestimate the fluxes (negative data points below the 1:1 line). In contrast, the application of a deadband ($H_{REA} = 0.6$) tends to slightly underestimate the turbulent fluxes, and yields a few outliers possibly due to the reduced amount of data used to calculate the updraft and downdraft differences.

4 Conclusions

For operational purposes, the use of temperature or water vapour concentration as a proxy scalar to derive the b factor is not found to be favourable over a constant parameterized b value. This is not surprising because of an overall low and varying scalar similarity (cf. Fig. 3). Considering the results presented in this study, we suggest deriving a theoretical b factor from a parameterization that includes a stability dependence (e.g. Ammann and Meixner 2002), use a dynamic deadband in the range $H_{REA} = 0.6$ to 0.8, and calculate the deadband effect according to Eq. 11 with $c = 0.378$ and $a = 2.300$. Due to the strong dependence of hyperbolic REA on scalar similarity (e.g. Ruppert et al. 2006), it is not recommended using a hyperbolic deadband definition with aerosol flux measurements. Even the use of aerosol number concentration as a proxy scalar for size-segregated or chemically resolved aerosol fluxes by REA may not be advantageous over the suggested theoretical b value. This should be investigated in future studies when direct eddy-covariance measurements of these aerosol fluxes are available. We also encourage analyzing the similarity of aerosol number concentration and potential proxy scalars over surfaces with scalar source/sink distributions different from this study, e.g. over the ocean or in urban areas.

Finally, REA simulations as a post-processing procedure of eddy-covariance measurements as presented here or in Pryor et al. (2007) can be a valuable tool for evaluating high-frequency data quality and the uncertainty of the resulting flux estimates.

Acknowledgements The authors would like to thank NCAR/EOL staff for their expertise and efforts in providing the turbulence measurements during CHATS. AH was supported by a research fellowship of the German Research Foundation DFG (HE-5214/1-1). Funding from the BEACHON project of The Institute for Integrative and Multidisciplinary Earth Studies (TIIMES) is gratefully acknowledged. The National Center for Atmospheric Research is funded by the National Science Foundation.

References

Ammann C, Meixner FX (2002) Stability dependence of the relaxed eddy accumulation coefficient for various scalar quantities. J Geophys Res 107. doi:10.1029/2001JD000649

Andreas EL, Hill RJ, Gosz JR, Moore DI, Otto WD, Sarma AD (1998) Stability dependence of the eddy-accumulation coefficients for momentum and scalars. Boundary-Layer Meteorol 86:409–420

Aubinet M, Heinesch B, Yernaux M (2003) Horizontal and vertical CO_2 advection in a sloping forest. Boundary-Layer Meteorol 108:397–417

Baldocchi D, Falge E, Gu L, Olson R, Hollinger D, Running S, Anthoni P, Bernhofer C, Davis K, Evans R, Fuentes J, Goldstein A, Katul G, Law B, Lee X, Malhi Y, Meyers T, Munger W, Oechel W, Paw UKT, Pilegaard K, Schmid HP, Valentini R, Verma S, Vesala T, Wilson K, Wofsyn S (2001) FLUXNET: a new tool to study the temporal and spatial variability of ecosystem-scale carbon dioxide, water vapor, and energy flux densities. Bull Am Meteorol Soc 82:2415–2434

Bowling DR, Delany AC, Turnipseed AA, Baldocchi DD, Monson RK (1999) Modification of the relaxed eddy accumulation technique to maximize measured scalar mixing ratio differences in updrafts and downdrafts. J Geophys Res 104:9121–9133

Businger JA, Oncley SP (1990) Flux measurement with conditional sampling. J Atmos Ocean Tech 7:349–352

Buzorius G, Rannik Ü, Mäkelä JM, Vesala T, Kulmala M (1998) Vertical aerosol particle fluxes measured by eddy-covariance technique using condensational particle counter. J Aerosol Sci 29:157–171

Buzorius G, Rannik Ü, Nilsson ED, Vesala T, Kulmala M (2003) Analysis of measurement techniques to determine dry deposition velocities of aerosol particles with diameters less than 100 nm. J Aerosol Sci 34:747–764

Desjardins RL (1977) Description and evaluation of sensible heat flux detector. Boundary-Layer Meteorol 11:147–154

Foken T, Dlugi R, Kramm G (1995) On the determination of dry deposition and emission of gaseous compounds at the biosphere–atmosphere interface. Meteorol Z 4:91–118

Gallagher MW, Beswick KM, Duyzer J, Westrate H, Choularton TW, Hummelshoj P (1997) Measurements of aerosol fluxes to Speulder forest using a micrometeorological technique. Atmos Environ 31:359–373

Gaman A, Rannik Ü, Aalto P, Pohja T, Siivola E, Kulmala M, Vesala T (2004) Relaxed eddy accumulation system for size-resolved aerosol particle flux measurements. J Atmos Ocean Tech 21:933–943

Gao W (1995) The vertical change of coefficient b, used in the relaxed eddy accumulation method for flux measurement above and within a forest canopy. Atmos Environ 29:2339–2347

Grönholm T, Aalto PP, Hiltunen V, Rannik Ü, Rinne J, Laakso L, Hyvönen S, Vesala T, Kulmala M (2007) Measurements of aerosol particle dry deposition velocity using the relaxed eddy accumulation technique. Tellus B 59:381–386

Held A, Klemm O (2006) Direct measurement of turbulent particle exchange with a twin CPC eddy covariance system. Atmos Environ 40:S92–102

Held A, Hinz K-P, Trimborn A, Spengler B, Klemm O (2003) Towards direct measurement of turbulent vertical fluxes of compounds in atmospheric aerosol particles. Geophys Res Lett 30:2016. doi:10.1029/2003GL017854

Held A, Nowak A, Birmili W, Wiedensohler A, Forkel R, Klemm O (2004) Observations of particle formation and growth in a mountainous forest region in Central Europe. J Geophys Res 109:D23204. doi:10.1029/2004JD005346

Held A, Nowak A, Wiedensohler A, Klemm O (2006) Field measurements and size-resolved model simulations of turbulent particle transport to a forest canopy. J Aerosol Sci 37:786–798

Hicks BB, McMillen RT (1984) A simulation of the eddy accumulation method for measuring pollutant fluxes. J Appl Meteorol 23:637–643

Horst TW (1997) A simple formula for attenuation of eddy fluxes measured with first-order-response scalar sensors. Boundary-Layer Meteorol 82:219–233

Kaimal JC, Wyngaard JC, Izumi Y, Cote OR (1972) Spectral characteristics of surface-layer turbulence. Q J Roy Meteorol Soc 98:563–589

Katul GG, Hsieh C-I (1999) A note on the flux-variance similarity relationships for heat and water vapour in the unstable atmospheric surface layer. Boundary-Layer Meteorol 90:327–338

Katul GG, Finkelstein PL, Clarke JF, Ellestad TG (1996) An investigation of the conditional sampling method used to estimate fluxes of active, reactive, and passive scalars. J Appl Meteorol 35:1835–1845

Klemm O, Held A, Forkel R, Gasche R, Kanter H-J, Rappenglück B, Steinbrecher R, Müller K, Plewka A, Cojocariu C, Kreuzwieser J, Valverde-Canossa J, Schuster G, Moortgat GK, Graus M, Hansel A (2006) Experiments on forest/atmosphere exchange: Climatology and fluxes during two summer campaigns in NE Bavaria. Atmos Environ 40:S3–20

Lee X (1998) On micrometeorological observations of surface-air exchange over tall vegetation. Agric Forest Meteorol 91:39–49

Meyers TP, Luke WT, Meisinger JJ (2006) Fluxes of ammonia and sulfate over maize using relaxed eddy accumulation. Agric Forest Meteorol 136:203–213

Myles L, Meyers TP, Robinson L (2007) Relaxed eddy accumulation measurements of ammonia, nitric acid, sulfur dioxide and particulate sulfate dry deposition near Tampa, FL, USA. Environ Res Lett 2. doi:10.1088/1748-9326/2/3/034004

Nemitz E, Williams PI, Theobald MR, McDonald AD, Fowler D, Gallagher MW (2001) Application of two micrometeorological techniques to derive fluxes of aerosol components above a city. In Midgley PM, Reuther M, Williams M (eds) Proceedings of EUROTRAC Symposium 2000. Springer, Berlin, 278 pp

Nemitz E, Jimenez JL, Huffman JA, Ulbrich IM, Canagaratna MR, Worsnop DR, Guenther AB (2008) An eddy-covariance system for the measurement of surface/atmosphere exchange fluxes of submicron aerosol chemical species—First application above an urban area. Aerosol Sci Technol 42:636–657

Norris SJ, Brooks IM, de Leeuw G, Smith MH, Moerman M, Lingard JJN (2008) Eddy covariance measurements of sea spray particles over the Atlantic Ocean. Atmos Chem Phys 8:555–563

Oncley SP, Delany AC, Horst TW, Tans PP (1993) Verification of flux measurement using relaxed eddy accumulation. Atmos Environ 27:2417–2426

Pattey E, Desjardins RL, Rochette P (1993) Accuracy of the relaxed eddy accumulation technique, evaluated using CO_2 flux measurements. Boundary-Layer Meteorol 66:341–355

Pearson RJ, Oncley SP, Delany AC (1998) A scalar similarity study based on surface layer ozone measurements over cotton during the California Ozone Deposition Experiment. J Geophys Res 103:18919–18926

Pryor SC, Larsen SE, Sørensen LL, Barthelmie RJ, Grönholm T, Kulmala M, Launiainen S, Rannik Ü, Vesala T (2007) Particle fluxes over forests: Analyses of flux methods and functional dependencies. J Geophys Res 112:D07205. doi:10.1029/2006JD008066

Ruppert J, Thomas C, Foken T (2006) Scalar similarity for relaxed eddy accumulation methods. Boundary-Layer Meteorol 120:39–63

Schery SD, Wasiolek PT, Nemetz BM, Yarger FD, Whittlestone S (1998) Relaxed eddy accumulator for flux measurement of nanometer-size particles. Aerosol Sci Technol 28:159–172

Wilczak JM, Oncley SP, Stage SA (2001) Sonic anemometer tilt correction algorithms. Boundary-Layer Meteorol 99:127–150

Willeke K, Baron PA (1996) Aerosol measurement: principles, techniques, and applications. VanNostrand Reinhold, New York, p 876

Wyngaard JC, Moeng C-H (1992) Parameterizing turbulent diffusion through the joint probability density. Boundary-Layer Meteorol 60:1–13